A Kinetic and Allosteric Model for the Acetylcholine Transporter-Vesamicol Receptor in Synaptic Vesicles†

Ben A. Bahr,‡ Edward D. Clarkson, Gary A. Rogers, Krystyna Noremberg, and Stanley M. Parsons*
Department of Chemistry and the Neuroscience Research Institute, University of California, Santa Barbara, California 93106
Received October 28, 1991; Revised Manuscript Received March 30, 1992

ABSTRACT: The ligand binding relationship between the acetylcholine transporter (AcChT) and the vesamicol receptor (VR) and the kinetics of active transport were studied in synaptic vesicles purified from the *Torpedo* electric organ using analogues of AcCh and vesamicol. Methoxyvesamicol, which should exhibit better equilibration properties for kinetics measurements than the more potent parent, inhibits active transport in a nonlinear noncompetitive manner. AcCh analogues competitively inhibit binding of [^{3}H]vesamicol with higher affinity in hyposmotically lysed vesicle ghosts than in intact vesicles, apparently due to removal of a competing internal, osmotically active factor. AcCh and actively transported analogues of AcCh that are up to 57% larger in van der Waals volume exhibit up to a 200-fold ratio for the dissociation constant measured by inhibition of vesamicol binding to ghosts (K_{IA}^g) compared to the Michaelis constant for transport (K_M) or the IC_{50} value for inhibition of [^{3}H]AcCh active transport. In contrast, two AcCh analogues that are about 120% larger and that almost surely are not transported exhibit a K_{IA}^g/IC_{50} ratio of about 1. The data demonstrate that the vesamicol family of compounds binds to an allosteric site in the AcChT. Initiation of active transport has no apparent effect on the affinities of vesamicol and AcCh analogues, which suggests that most of the AcChT-VR in purified vesicles is transport incompetent. Vesicle ghosts actively transport [^{3}H]AcCh nearly as well as intact vesicles, which suggests that internal factor does not affect transport-competent AcChT-VR. A kinetics model is proposed that predicts that AcCh analogues exhibiting a K_{IA}^g/IC_{50} ratio significantly greater than 1 are actively transported. Some of the microscopic constants in the model are estimated. The AcChT binds AcCh very weakly with a dissociation constant of about 20-50 mM, but it transports substrates rapidly in a process exhibiting remarkably little selectivity for the detailed shape and volume of the transported ion.

The acetylcholine (AcCh)[1] active transport system of synaptic vesicles includes a transporter and a cytoplasmically oriented (Kornreich & Parsons, 1988) binding site for the drug (-)-*trans*-2-(4-phenylpiperidino)cyclohexanol (vesamicol), which inhibits AcCh uptake in an apparently noncompetitive manner (Bahr & Parsons, 1986a). A vacuolar-type ATPase pumps protons into the vesicles, and the AcCh transporter (AcChT) probably exchanges the stored protons for cytoplasmic AcCh, thus effecting AcCh uptake (Marshall & Parsons, 1987). Extensive structure-activity studies on vesamicol (Rogers et al., 1989) and AcCh (Rogers & Parsons, 1989) analogues indicate that different types of contacts with the respective binding sites are involved. It is likely, therefore, that the binding sites are not identical. The vesamicol binding site lies either in the AcChT as an allosteric site (model 1) or in a separate protein that acts via an unknown mechanism to inhibit transport (model 2; Marshall & Parsons, 1987).

It has been difficult to distinguish between the models because of a number of complexities. Heterogeneity and preparation to preparation variation in the quantitative properties of the system, such as the amounts of the VR and AcCh active transport, are usual (Anderson et al., 1986; Bahr & Parsons, 1986a,b; Gracz et al., 1988). Occupation of only a fraction of the VR is sufficient to achieve complete inhibition of active transport (Kaufman et al., 1989). This phenomenon is reminescent of the spare receptor concept and could imply indirect linkage between the AcChT and the VR. Although vesamicol is the paradigm drug for inhibition of AcCh storage, many other drugs, such as chloroquine and levorphanol, are less potent inhibitors (Anderson et al., 1983). They are competitive with respect to vesamicol, which suggests that they bind to the VR (Kaufman et al., 1989). This is perplexing, as structurally dissimilar drugs would not likely induce the same propagated conformational change needed to inhibit the AcChT in the conventional model of allostery. Further complicating the situation is the existence of an internal factor, releasable by hyposmotic lysis, that inhibits the binding of AcCh and vesamicol, apparently by means of a transmembrane conformational change (Noremberg & Parsons, 1989).

Recently, AcCh was found to inhibit binding of vesamicol, but the equilibrium dissociation constant for AcCh was so high

† This research was supported by Grant NS15047 from the National Institute of Neurological Disorders and Stroke, Grant BNS 06431 from the National Science Foundation, and a grant from the Muscular Dystrophy Association.

* To whom correspondence should be addressed.
‡ Present address: Department of Psychobiology, Center for the Neurobiology of Learning and Memory, University of California, Irvine, CA 92717-3800.

[1] Abbreviations: AcCh, acetylcholine; AcChT, acetylcholine transporter; vesamicol, (-)-*trans*-2-(4-phenylpiperidino)cyclohexanol; VR, vesamicol receptor; IC_{50}, concentration of a ligand giving 50% inhibition of trace [^{3}H]AcCh active transport; K_{IA}^g, equilibrium dissociation constant of an AcChT·AcCh analogue complex in vesicle ghosts measured by competition against binding of [^{3}H]vesamicol; K_{IA}, equilibrium dissociation constant of an AcChT·AcCh analogue complex in intact vesicles measured by competition against binding of trace [^{3}H]vesamicol; K_{IV}, equilibrium dissociation constant of a VR·vesamicol analogue complex in intact vesicles measured by competition against binding of trace [^{3}H]vesamicol; HEPES, *N*-(2-hydroxyethyl)piperazine-*N*′-2-ethanesulfonic acid; EDTA, ethylenediaminetetraacetic acid; EGTA, ethylene glycol bis(β-aminoethyl ether)-*N*,*N*,*N*′,*N*′-tetraacetic acid; K_{DV}, equilibrium dissociation constant of the VR·vesamicol complex measured by direct titration with [^{3}H]vesamicol; B_{max}, picomoles of VR sites per milligram of protein; *n*, Hill coefficient.

0006-2960/92/0431-5752$03.00/0

in this measurement (18 mM) that it could not be determined whether the interaction is competitive or noncompetitive (Bahr & Parsons, 1989; Noremberg & Parsons, 1989; Parsons et al., 1988). Also, the affinity is so much lower than the active transport Michaelis constant (K_M = 0.3 mM) that it seemed likely that a different site (for example, a regulatory site in a separate VR) or a different form of the transporter binding site was involved (Noremberg & Parsons, 1989). ATP had no effect on the inhibition, which suggests that AcCh binding observed in this manner is not to the transporter. Thus, bidirectional effects consistent with an allosteric relationship have been observed (namely, vesamicol inhibits AcCh active transport noncompetitively and AcCh inhibits vesamicol binding), but many quantitative and qualitative aspects of the coupling between AcCh and vesamicol binding sites are not easily reconciled with an allosteric model.

Experiments designed to distinguish between the models and to rationalize the complexity are reported in this paper. Highly purified synaptic vesicles obtained from *Torpedo* electric organ were studied. Newly synthesized AcCh and vesamicol analogues were utilized to probe the relationships among the several binding sites more effectively than was possible with the parent compounds. The interpretation of the data has been aided greatly by our recent demonstration that surprisingly large and structurally diverse AcCh analogues are actively transported with V_{max} values similar to that of AcCh itself (Clarkson et al., 1992). The observation of two apparent affinities of vesicles for all transported molecules, depending upon the assay method, contrasted with a single affinity for larger AcCh analogues that are not transported also was key to the analysis. A new kinetics model of the system that can explain apparent low- and high-affinity AcCh binding sites and the relationship of each to the VR is proposed. The model posits extraordinary active transport properties for the AcChT. Three papers following this one demonstrate that the system also is associated with an unexpected macromolecular structure (Bahr & Parsons, 1992; Rogers & Parsons, 1992; Bahr et al., 1992).

Materials and Methods

Materials. Torpedo californica electric organ VP_1 synaptic vesicles were isolated as described by Noremberg and Parsons (1989). This involves differential sedimentation velocity pelleting, equilibrium buoyant density centrifugation, and size exclusion chromatography of vesicles in isosmotic glycine–sucrose solutions. [^{3}H]Vesamicol (27 Ci/mmol) was purified as described (Bahr & Parsons, 1986b). The nonradioactive AcCh analogues utilized in this study were synthesized as described (Rogers & Parsons, 1989). They were (±)-*cis*,-*trans*-1-benzyl-1-methyl-3-acetoxypyrrolidinium bromide (analogue 14),[2] (±)-1,1-dimethyl-3-benzoyloxypyrrolidinium iodide (analogue 15), methyl 1,1-dimethylisonipecotate iodide (analogue 21), *cis*-benzyl 1-benzyl-1-methylisonipecotate bromide (analogue 23), and *cis*,*trans*-cyclopentylmethyl 1-benzyl-1-methylisonipecotate bromide (analogue 25). *trans*-6-Methoxyvesamicol was synthesized as described (Rogers et al., 1989). [^{3}H]Analogues 14 and 15 were synthesized as described (Clarkson et al., 1992). [^{3}H]AcCh chloride (100 mCi/mmol) was obtained from Du Pont, Inc.

Ligand Binding and Uptake by Intact Vesicles. Purified vesicles were concentrated and transferred into titration buffer (100 mM HEPES, 700 mM glycine, 1 mM EDTA, 1 mM EGTA adjusted to pH 7.8 with KOH) by using a Centricon 30 centrifugal ultrafiltration device (Amicon Corp.). Concentrated vesicles were incubated with 0.15 mM diethyl-*p*-nitrophenyl phosphate (paraoxon) for 1 h at 23 °C and then mixed with other substrates. Further incubation was done as described in the figure legends, and bound radioactivity was determined using the filter assay described below.

Ligand Binding by Vesicle Ghosts. Purified vesicles were concentrated by ultracentrifugal pelleting. The pelleted vesicles were resuspended at 1.54 mg of protein/mL of buffer containing 100 mM HEPES, 10 mM EDTA, 1 mM EGTA, and 0.02% (w/v) NaN_3 that was adjusted to pH 7.8 with KOH and then incubated with paraoxon as above. This procedure causes hyposmotic lysis of the vesicles. The suspension was diluted 10-fold into 25 mM HEPES buffer (adjusted to pH 7.8 with KOH) containing [^{3}H]vesamicol and the competing ligand. The mixture was equilibrated at 23 °C for 60 min before measuring bound [^{3}H]vesamicol.

AcCh Active Transport by Vesicle Ghosts. Purified vesicles were concentrated by ultracentrifugal pelleting and resuspended in titration buffer at 10 mg of protein/mL. Ten microliters was mixed with 700 μL of titration buffer (sample A), 500 μL of water (sample B), or 500 μL of water (sample C) and incubated 20 min at 0 °C. Sample B was returned to titration buffer by addition of 135 μL of 5.2-fold concentrated titration buffer and 65 μL of titration buffer. Sample C was made up to 700-μL total volume with 50 μL of titration buffer and 150 μL of water. Identical samples containing 1.7 μM vesamicol also were prepared. Vesicles were treated with paraoxon as above, mixed with substrates, and incubated as described in the figure legends. Bound [^{3}H]AcCh was determined using the filter assay described below.

Assays and Data Analysis. [^{3}H]Vesamicol, [^{3}H]AcCh, [^{3}H]analogue 14, or [^{3}H]analogue 15 was incubated with ghosts or intact vesicles as described in figure legends. Samples (50–100 μL) were filtered with suction-assistance through polyethylenimine-coated (0.5% for 2 h, then rinsed with water) glass-fiber filters (type GF/F; Whatman Corp., Hillsboro, OR) that then were washed quickly with four sequential ice-cold 1-mL volumes of the same buffer utilized in the incubation. Filters were prewashed immediately prior to sampling. Filter-bound tritium was measured by liquid scintillation spectroscopy. To facilitate solubilization of [^{3}H]AcCh and [^{3}H]analogues 14 and 15, scintillation fluid contained 10% water. Nonspecific binding was defined as the amount of radioactivity taken up in the presence of an excess of nonradioactive vesamicol. Results usually are expressed as specifically bound or transported radioactivity, which equals the difference between the total bound and nonspecifically bound radioactivity. When free [^{3}H]vesamicol was the independent variable, it was calculated by subtraction of bound [^{3}H]vesamicol from total [^{3}H]vesamicol. Parameters were estimated by nonlinear regression analysis using equations that were simultaneously fit to the data where appropriate with the software MINSQ (Micromath Scientific Software, Salt Lake City, UT). Best parameter values are quoted ±1 SD. Protein concentration was determined with a bovine serum albumin standard using the Bradford (1976) assay or the BCA assay (Pierce Chemical Co., Rockford, IL).

Results

Methoxyvesamicol Is a Noncompetitive Inhibitor of AcCh Active Transport. For the reason given under Discussion, inhibition of [^{3}H]AcCh active transport by *trans*-6-methoxyvesamicol [analogue 55 in Rogers et al. (1989)] was studied. The initial velocity inhibition data for intact vesicles (Figure 1) are fit well by a nonlinear noncompetitive inhibition

[2] In Rogers and Parsons (1989) the *E*,*Z* nomenclature was used to designate *trans*- and *cis*-isomers.

Table I: Structures of AcCh Analogues

analogue[a]	structure[b]	volume[c] (Å^3)	analogue	structure	volume (Å^3)
AcCh	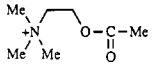	122	14[d]	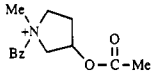	192
21	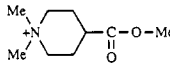	143	25[d]	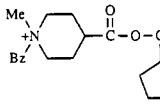	266
15	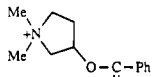	178	23[e]	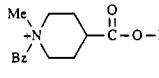	268

[a] Analogue numbers are taken from Rogers and Parsons (1989). [b] Bz = benzyl, Me = methyl, and Ph = phenyl. [c] van der Waals volumes were calculated with the CHEM-X computer program (Chemical Design, Ltd., Oxford). [d] cis and trans mixture. [e] cis.

model (Cleland, 1979) in which we assume that binding of methoxyvesamicol is cooperative (Gracz et al., 1988). The competitive and linear models fit much worse by the *F*-test criterion ($P < 0.001$ and < 0.005, respectively). The regression values obtained were as follows: Michaelis transport dissociation constant (K_M) = 380 ± 40 μM; maximal velocity (V_{max}) = 2.7 ± 0.1 nmol of AcCh/(mg·min); methoxyvesamicol intercept (K_{ii}) and slope (K_{is}) inhibition constants = 6.2 ± 0.8 μM and 2.7 ± 0.5 μM, respectively; and Hill coefficient (n) for methoxyvesamicol = 1.3 ± 0.1 (Table II). The names "intercept and slope inhibition constants" denote the effects of the inhibitor on the double-reciprocal plot (Figure 1, inset). The B_{max} for the VR was estimated with nearly saturating [^{3}H]vesamicol as 500 pmol/mg of protein.

Methoxyvesamicol Is a Noncompetitive Inhibitor of Analogue 14 and 15 Active Transport. AcCh analogues 14 and 15 recently were shown to be actively transported with V_{max} values that were the same as or somewhat less than (depending on the preparation of vesicles utilized) the value for AcCh itself (Clarkson et al., 1992). The structures of these analogues are shown in Table I. Full initial velocity inhibition studies similar to that of Figure 1 were carried out on them. Methoxyvesamicol was a noncompetitive nonlinear inhibitor of uptake of both analogues (Table II). In these experiments, the V_{max} values for active transport of the analogues were the same as for AcCh in the same preparation of vesicles, and the K_M values were similar to the IC_{50} values that previously had been measured by inhibition of trace [^{3}H]AcCh active transport (Table III). B_{max} values for the VR also were measured in the same preparations of vesicles (Table II).

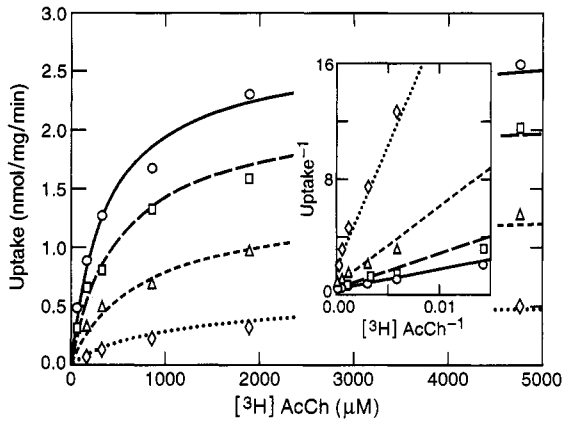

FIGURE 1: Methoxyvesamicol is a noncompetitive nonlinear inhibitor of AcCh active transport. Intact synaptic vesicles were introduced into premixed solutions resulting in final concentrations of MgATP at 10 mM, $MgCl_2$ at 2 mM, the indicated concentration of [^{3}H]AcCh chloride, and methoxyvesamicol at 0 (○), 2 (□), 6 (△), or 18 μM (◇). All components were in titration buffer, and incubation was carried out at 23 °C for 8 min at a vesicle concentration of 0.15 mg of protein/mL. Transported [^{3}H]AcCh was determined by the filter assay. All data shown are the averages of triplicates with a typical relative range of less than 10%. A noncompetitive model, given under Results, was fitted simultaneously to generate the lines shown, and the parameters are given in Table II. Similar results were obtained in two other experiments.

AcCh Analogues Inhibit Vesamicol Binding to Intact Synaptic Vesicles. The above AcCh analogues and others that systematically explored the consequences of appendent steric bulk all were found to inhibit binding of trace [^{3}H]vesamicol as AcCh does. K_{IA} values were determined for the effect. The subscript I indicates that the value is an equilibrium inhibition constant and the subscript A that the value is for a member of the AcCh ligand family. The structures and van der Waals volumes of all of the analogues studied here are listed in Table I. Thus, analogue 21 adds only 17% more bulk; analogue 15 adds 46% more bulk, mostly at the acyl end; analogue 14 adds 57% more bulk, mostly at the ammonium end; and analogues

Table II: Macroscopic Regression Parameters for Active Transport, Inhibition by Methoxyvesamicol, and Binding of [^{3}H]Vesamicol[a]

AcCh analogue[b]	K_M (μM)	V_{max} analogue [nmol/(mg·min)]	V_{max} AcCh [nmol/(mg·min)]	B_{max} VR (pmol/mg)	K_{ii} (μM)	K_{is} (μM)	n
AcCh	380 ± 40		2.7 ± 0.1	500	6.2 ± 0.8	2.7 ± 0.5	1.3 ± 0.1
15	53 ± 8	1.8 ± 0.1	1.6 ± 0.1	580	11 ± 1	8.5 ± 2.3	1.6 ± 0.2
14	84 ± 20	0.68 ± 0.06	0.65 ± 0.01	416	13 ± 4	5.4 ■ 1.6	1.3 ± 0.2

[a] Parameters are defined in the text. Values for AcCh analogues and methoxyvesamicol were obtained from experiments of the type shown in Figure 1. [b] Structures of the analogues are shown in Table I.

Table III: Competitive Inhibition by AcCh Analogues

analogue[a]	K_{IA} (μM)[b]	K_{IA}^g (μM)[c]	IC_{50} (μM)[d]	K_{IA}^g/IC_{50}[e]	K_{IA}^g/K_M[e]
AcCh	440 000 ± 120 000	49 000 ± 14 000	290 ± 20	200	100
21	660 000 ± 180 000	5900 ± 2500	140 ± 15	40	NT[f]
15	19 000 ± 3000	710 ± 340	33 ± 3	20	10
14	NT[f]	1700 ± 500	30 ± 10	60	20
25	70 ± 9	1.2 ± 0.3	0.58 ± 0.16	2	NT[f]
23	230 ± 40	1.7 ± 0.6	1.7 ± 0.4	1	NT[f]

[a] Structures of the analogues are shown in Table I. [b] The K_{IA} values for inhibition of trace [^{3}H]vesamicol binding to intact, fresh vesicles by the analogues were determined by regression analyses of the type shown in Figure 2. [c] The K_{IA}^g values for inhibition of [^{3}H]vesamicol binding to vesicle ghosts by the analogues were determined by regression analyses of the type shown in Figure 3. In all cases, the model for competitive inhibition of binding fit the data well. These studies consistently assigned the vesamicol·VR complex a macroscopic dissociation constant (K_{DV}) of 35–50 nM. Values are given to two significant figures. [d] IC_{50} values for inhibition of AcCh active transport by the analogues are taken from Rogers and Parsons (1989). [e] Ratios are rounded to one significant figure. [f] Not tested.

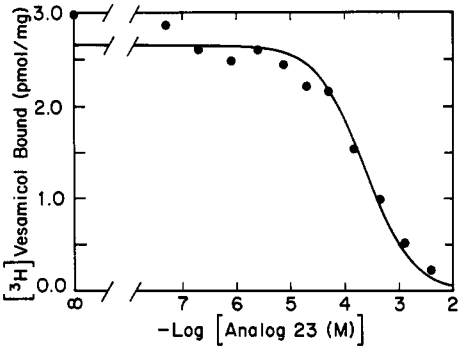

FIGURE 2: AcCh analogues inhibit vesamicol binding to intact synaptic vesicles. Synaptic vesicles were introduced into premixed solutions yielding 5 nM [^{3}H]vesamicol and the indicated concentration of AcCh analogue 23. All components were in titration buffer, and incubation was carried out at 23 °C for 30 min at a vesicle concentration of 0.15 mg of protein/mL. Bound tritium was determined by the filter assay. All data shown are the averages of triplicates with a typical relative range of less than 10%. A hyperbolic curve was fitted to the data and graphed with respect to the negative logarithm base 10 of the analogue concentration. K_{IA}, the analogue 23 dissociation constant, is 230 ± 40 μM. Similar competition titrations were carried out with most of the AcCh analogues and AcCh, and the K_{IA} values determined are listed in Table III.

25 and 23 add 118% and 120% more bulk, respectively, distributed mostly to both ends. A displacement curve example for analogue 23 is shown in Figure 2, and the similarly derived K_{IA} values for all of the analogues are listed in Table III.

AcCh Analogs Are Potent, Competitive Inhibitors of Vesamicol Binding to Synaptic Vesicle Ghosts. AcCh analogues bind with higher affinities to vesicle ghosts than intact vesicles, just as AcCh does. The ghosts were produced by hyposmotic lysis, and they have been shown to spontaneously reseal right-side-out (Noremberg & Parsons, 1989). At constant pH, binding of vesamicol and AcCh analogues to either intact vesicles or ghosts is not sensitive to changes in buffer composition if membrane integrity is not further affected (data not shown). The greater affinities for ghosts made it easier to achieve concentrations of analogues that were sufficiently above their dissociation constants to distinguish between competitive and noncompetitive inhibition. Still, only analogues 23 and 25 bound with high enough affinity to conclude with good certainty that they are competitive. Only for these analogues could binding of [^{3}H]vesamicol be inhibited completely even at an otherwise saturating concentration. The results of the study with analogue 25 are shown in Figure 3, for which the dissociation constant K_{IA}^g was 1.2 ± 0.3 μM. The superscript g indicates that the value was obtained in vesicle ghosts. The values of K_{IA}^g similarly obtained for all of the AcCh analogues, based on a competitive analysis, are listed in Table III. There was no statistical justification for a noncompetitive term in the binding equation for any of the analogues.

The K_{IA}^g value for AcCh should be compared with the much lower K_M and previously measured IC_{50} values (Tables II and III). For any molecule that is transported, IC_{50} should equal K_M, as it does for AcCh itself. A 100–200-fold discrepancy between K_{IA}^g and K_M or IC_{50} exists for AcCh (Table III). Large discrepancies also exist for analogues 14 and 15 if K_{IA}^g values are compared to the K_M or IC_{50} values, and a large discrepancy exists for analogue 21 if K_{IA}^g is compared to IC_{50}. No significant discrepancies were found for analogues 23 and 25 in corresponding K_{IA}^g and IC_{50} values. The origin of the discrepancies will be discussed below.

Synaptic Vesicle Ghosts Actively Transport AcCh Almost as Well as Intact Vesicles Do. It was of interest to ask whether

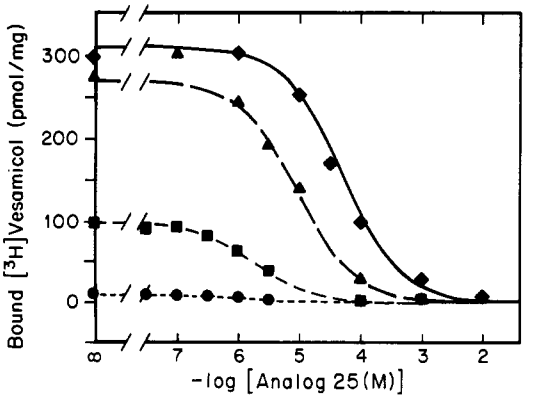

FIGURE 3: AcCh analogues are competitive inhibitors of vesamicol binding to synaptic vesicle ghosts. Ghosts (0.13 mg of protein/mL) prepared by hyposmotic lysis as described under Materials and Methods were equilibrated with 2 nM (●), 20 nM (■), 200 nM (▲), or 1 μM (◆) [^{3}H]vesamicol for 60 min at 23 °C in the presence of the indicated concentrations of analogue 25. Bound ^{3}H was determined by the filter assay. A simple linear competitive binding model was fitted simultaneously to the data to generate the lines shown that are graphed with respect to the negative logarithm base 10 of the analogue 25 concentration. K_{IA}^g, the AcCh analogue dissociation constant for ghosts, is 1.2 ± 0.3 μM; K_{DV}, the dissociation constant for vesamicol, is 40 ± 4 nM; and B_{max} is 317 ± 9 pmol/mg of protein. Similar competition titrations were carried out with the rest of the AcCh analogues and AcCh, and the K_{IA}^g values determined are listed in Table III.

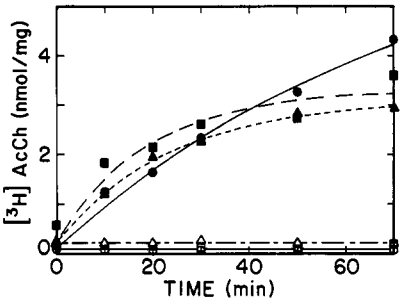

FIGURE 4: AcCh is actively transported by synaptic vesicle ghosts. Intact vesicles (●, ○), vesicle ghosts returned to the same buffer system (■, □), and vesicle ghosts in hyposmotic buffer (▲, △) were prepared as described under Materials and Methods. An ATP-regeneration system (100 μL) in titration buffer was added to 700 μL of vesicle sample to yield MgATP at 10 mM, $MgCl_2$ at 2 mM, potassium phosphoenolpyruvate at 10 mM, and pyruvate kinase (Sigma type III) at 10 μg/mL. The samples were incubated 1 min at 23 °C after which 10 μL of [^{3}H]AcCh in titration buffer was added to yield 125 μM. Total transported [^{3}H]AcCh was determined in duplicate (●, ■, ▲) and nonspecifically bound [^{3}H]AcCh in the presence of vesamicol in singlet (○, □, △) by the filter assay at the indicated times. Only the averages of the duplicates, which exhibited a relative range of less than 10% are shown.

formation of synaptic vesicle ghosts affects the active transport of [^{3}H]AcCh. For example, if a large fraction of the [^{3}H]-AcCh uptake arose by exchange with nonradiolabeled endogenous AcCh, a large decrease in uptake of [^{3}H]AcCh would occur. The time courses for vesamicol-sensitive uptake of subsaturating [^{3}H]AcCh by intact vesicles, ghosts, and ghosts returned to the same buffer environment as the intact vesicles are shown in Figure 4. The initial velocities were similar, and the extents of uptake by the vesicle ghosts after 70 min were similar. This result indicates that the internal contents of intact vesicles likely do not have a significant effect on either V_{max} or K_M, because at a subsaturating concentration of [^{3}H]AcCh the uptake would respond to a change in either parameter.

Effects of Transport Activation on Ligand Binding. Acidification of the vesicle interior and establishment of the

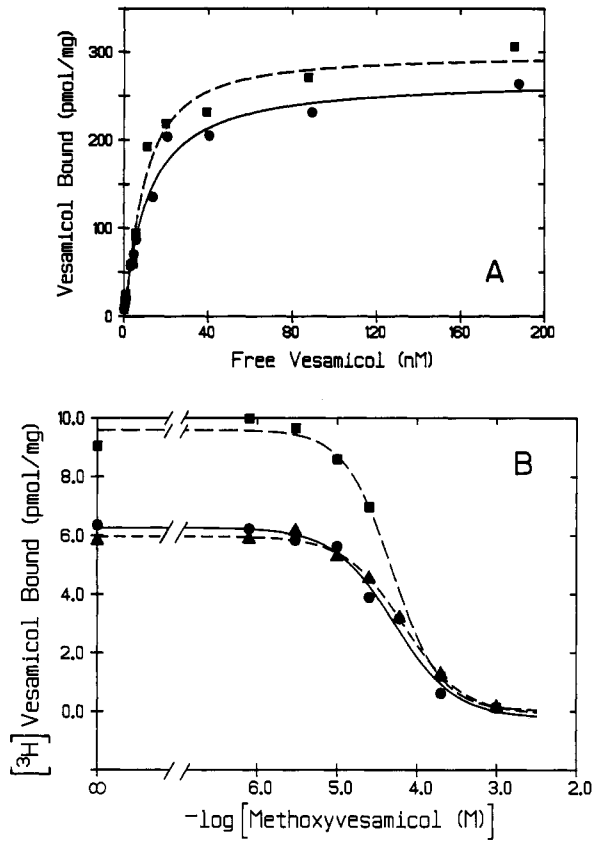

FIGURE 5: Effects of transport activation on ligand binding. (Panel A) Effect of MgATP on vesamicol binding. Intact vesicles at 0.05 mg of protein/mL in chelator-free titration buffer were incubated 30 min at 23 °C in different concentrations of [^{3}H]vesamicol and either 1 mM EGTA plus 1 mM EDTA (■) or 10 mM MgATP (●). Bound [^{3}H]vesamicol was determined by the filter assay. All data shown are the averages of triplicates with a relative range of less than 5%. The equation Bound = $B_{max}K_{DV}{}^nV^n/(K_{DV}{}^n + V^n)$ was fitted to the data to yield the lines shown, where B_{max} is the concentration of VR, K_{DV} is the VR·vesamicol dissociation constant, V is the free vesamicol concentration, and n is the Hill coefficient. In the absence of MgATP, the best parameters are K_{DV} = 9.5 ● 1.5 nM, B_{max} = 296 ± 17 pmol/mg, and n = 1.3 ± 0.2. In the presence of MgATP, K_{DV} = 11.3 ± 1.8 nM, B_{max} = 268 ± 15 pmol/mg, and n = 1.1 ± 0.1. Similar results were obtained in six other experiments. (Panel B) Inhibition of [^{3}H]vesamicol binding by methoxyvesamicol. Intact synaptic vesicles were introduced into premixed solutions, yielding final concentrations of [^{3}H]vesamicol at 5 nM, $MgCl_2$ at 2 mM, and AcCh chloride at 3 mM (■); Na_2ATP at 10 mM and $MgCl_2$ at 12 mM (●); or Na_2ATP at 10 mM, $MgCl_2$ at 12 mM, and AcCh chloride at 3 mM (▲). All components were in titration buffer, and incubation was carried out at 23 °C for 30 min at a vesicle concentration of 0.15 mg of protein/mL and the indicated methoxyvesamicol concentrations. Bound [^{3}H]vesamicol was determined by the filter assay. All data shown are the averages of triplicates with a typical relative range of less than 10%. The equation Bound = $B_0K_{IV}{}^n/(K_{IV}{}^n + MV^n)$ was fitted to the data. MV is the methoxyvesamicol concentration, and B_0 is the amount of bound [^{3}H]vesamicol in the absence of MV. The other symbols are defined elsewhere. The results are graphed with respect to the negative logarithm base 10 of MV. Regression values are K_{IV} = 51 ± 11 μM and n = 1.1 ± 0.3 for methoxyvesamicol in the presence of AcCh (■); K_{IV} = 49 ± 10 μM and n = 1.4 ± 0.3 for methoxyvesamicol in the presence of ATP (●); and K_{IV} = 68 ± 9 μM and n = 1.2 ± 0.2 for methoxyvesamicol in the presence of ATP plus AcCh (▲). Similar results were obtained in one other experiment.

transmembrane, interior positive electrical potential might alter the conformation of the AcChT and VR in a manner that would affect the binding of the ligands. However, MgATP variably affected only one parameter of the VR saturation curve in intact vesicles (Figure 5A). There was no change in the dissociation constant (K_{DV}) or n. The subscript D indicates that the value is a directly measured constant, and the subscript V indicates that the value is for a member of the vesamicol ligand family. There was a small decrease in B_{max} in this preparation of vesicles, and other preparations exhibited 0–35% decreases. MgATP had no significant effect on the ability of analogue 23 to inhibit the binding of trace [^{3}H]-vesamicol to ghosts (data not shown).

It was of interest to compare the kinetically determined values K_{is} and K_{ii} with equilibrium measurements of the affinity of the VR for methoxyvesamicol. This was done by competition against binding of trace [^{3}H]vesamicol in the absence and presence of MgATP and sufficient AcCh to nearly saturate active transport (Figure 5B). The presence of active transport conditions did not much affect the affinity for methoxyvesamicol, but the amount of binding of [^{3}H]vesamicol was reduced about 30%. This is due to the MgATP effect (above). The regression values obtained for the displacement curves were as follows: resting vesicles in AcCh, dissociation constant (K_{IV}) = 51 ± 11 μM; vesicles in MgATP, K_{IV} = 49 ± 10 μM; and vesicles in MgATP plus AcCh, K_{IV} = 68 ± 9 μM. The value of n did not differ significantly from 1 in all cases. Thus, no significant effect on the binding of methoxyvesamicol was observed as a result of initiation of active transport. A higher concentration of methoxyvesamicol was required to saturate the VR compared to that required to inhibit active transport.

Discussion

Each type of kinetic or equilibrium inhibition or dissociation constant measured in these studies has been designated with a unique symbol in order to facilitate a precise analysis. Careful attention to the meaning of each symbol is required to follow the analysis. The same symbols are utilized in the following papers of this series.

One part of this study was a confirmation of an older result obtained with vesamicol. Derivation of the usual initial velocity equations describing competitive and noncompetitive modes of inhibition is done with the assumption that the free inhibitor is in equilibrium with bound inhibitor. However, the half-life for self-exchange of vesamicol in the VR·vesamicol complex at 23 °C is 3.0 min (Bahr & Parsons, 1986b). This is comparable to the 8-min period that was used to obtain initial velocity data in the study that attempted to determine the kinetic mechanism for inhibition of AcCh active transport by vesamicol (Bahr & Parsons, 1986a). Slow dissociation of vesamicol could produce a noncompetitive inhibition pattern, even if the actual inhibition were competitive, because of incomplete relaxation to a new equilibrium after addition of [^{3}H]AcCh. To test whether this phenomenon had occurred, the experiment was repeated utilizing one of the lower affinity vesamicol analogues that recently became available (Rogers et al., 1989). A ligand that is an analogue of another and that binds more weakly often does so because it dissociates from the bound state more rapidly. *trans*-6-Methoxyvesamicol was chosen for this test because its IC_{50} value suggests that the dissociation rate constant is about 100-fold greater than that of vesamicol. This should be fast enough to ensure equilibration. The scatter in the replicate transport-inhibition data was reduced with methoxyvesamicol compared to vesamicol, and the noncompetitive kinetics relationship between the vesamicol family and inhibition of active transport of the AcCh family was confirmed. The remainder of the discussion will lead to a choice between models 1 and 2 for the AcChT and VR system and to a quantitative analysis of the favored model.

It is clear for the following two reasons that the vesamicol binding site lies within the AcChT. First, AcCh analogues 14 and 15 are actively transported while being probable com-

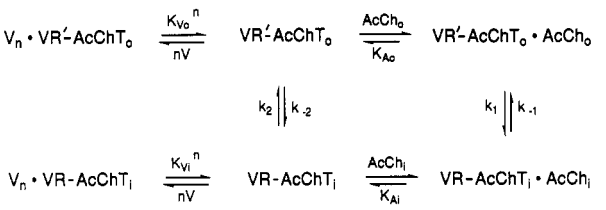

FIGURE 6: Kinetic model for the AcChT–VR. $AcCh_o$ is AcCh on the outside of the vesicle, V is vesamicol on the outside, $AcCh_i$ is on the inside, $VR'\text{–}AcChT_o$ is outwardly oriented empty transporter and empty VR, $VR'\text{–}AcChT_o\cdot AcCh_o$ is outwardly oriented loaded transporter and empty VR′, $VR\text{–}AcChT_i\cdot AcCh_i$ is inwardly oriented loaded transporter and empty VR, $VR\text{–}AcChT_i$ is inwardly oriented empty transporter and empty VR, $V_n\cdot VR\text{–}AcChT_i$ is inwardly oriented empty transporter with n molecules of vesamicol bound on the outside of the vesicle, and $V_n\cdot VR'\text{–}AcChT_o$ is outwardly oriented empty transporter with n molecules of vesamicol bound on the outside. Binding of AcCh is hypothesized to be at equilibrium outside and inside of the vesicle with dissociation constants of K_{Ao} and K_{Ai}, respectively. Vesamicol binding exhibits dissociation constants of K_{Vo} and K_{Vi} for outwardly or inwardly oriented transporter, respectively. In both cases the Hill coefficient is n. Reorientation of the AcCh binding site across the membrane in the "forward" direction resulting in cyclic uptake of AcCh occurs with rate constants k_1 and k_2. Reorientation in the "reverse" direction resulting in cyclic efflux of AcCh occurs with rate constants k_{-1} and k_{-2}.

petitive inhibitors of vesamicol binding. Second, AcCh analogue 23 is an equipotent competitive inhibitor of both AcCh active transport (Rogers & Parsons, 1989) and vesamicol binding to ghosts. All other data are consistent with this conclusion. Analogues 14, 15, 21, 23, and 25 are truely AcCh analogues because the structure–activity studies clearly distinguish the requirements for good binding to the AcCh and vesamicol sites and demonstrate that quaternary amino esters bind in a predictable manner to the AcCh site. We thus choose allosteric model 1 for the system, and we will refer to the AcChT–VR as a single complex. The challenge now is to explain quantitatively how the two ligand families exhibit a competitive binding relationship under equilibrium conditions, a noncompetitive kinetic relationship during active transport, and different apparent affinities depending on how the measurements are made. We deal later in the discussion with other complexities in the system.

A proposed kinetics scheme is shown in Figure 6. The outside or inside location of the transporter binding site and AcCh is denoted by the subscripts o or i, respectively. AcCh binding is hypothesized to be at equilibrium outside and inside of the vesicle, even during active transport, with microscopic dissociation constants of K_{Ao} and K_{Ai}, respectively. This is a reasonable assumption since AcCh binds relatively weakly. The reorientation of the transporter binding site across the membrane is hypothesized to be at steady state during active transport, with the microscopic rate constants in the indicated directions being k_1 and k_{-1} for the loaded transporter and k_2 and k_{-2} for the empty transporter. Values of K_{Ao}, K_{Ai}, k_1, and k_{-1} will be AcCh analogue-dependent.

In the analysis that follows, it is assumed that during active transport the same states exist as under equilibrium conditions, but at least one of the rates of transmembrane reorientation of the transporter is different. Vesamicol must bind to the outside (Kornreich & Parsons, 1988) of at least one of the four basic transporter states. This state cannot be $VR'\text{–}AcChT_o\cdot AcCh_o$ or $VR\text{–}AcChT_i\cdot AcCh_i$ because AcCh analogues (and by inference probably AcCh itself) are competitive inhibitors of vesamicol binding at equilibrium. It cannot be only $VR'\text{–}AcChT_o$ because vesamicol is a noncompetitive inhibitor of active transport. Thus, $VR\text{–}AcChT_i$ must be capable of binding vesamicol with microscopic equilibrium dissociation constant K_{Vi}. Vesamicol binding can be at equilibrium even during active transport as it forms an unproductive complex. Because vesamicol binding can be cooperative (Gracz et al., 1988) and a nonunitary Hill-type coefficient for transport inhibition by the vesamicol family was shown here to be statistically justified, the vesamicol binding step is postulated to be of order n. Moreover, as will be shown below, $VR'\text{–}AcChT_o$ must bind vesamicol with microscopic equilibrium dissociation constant K_{Vo}. This step will be assumed to be of order n as well. Because the scheme hypothesizes separate AcCh and vesamicol binding sites, it is consistent with the structure–activity data. Values of K_{Vi}, K_{Vo}, and n will be vesamicol analogue-dependent.

The complete steady-state rate expression for active transport of AcCh and inhibition of transport by vesamicol is derived in the Appendix. The expression can be simplified greatly. Because resealed vesicle ghosts transport AcCh to nearly the same extent as intact vesicles, either $K_{Ai} = \infty$ or $[AcCh_i] = 0$. This allows us to recast eq f of the Appendix into a macroscopic form that is experimentally accessible, namely, that

$$\frac{\text{rate}}{V_{max}} = \frac{[AcCh_o]}{K_M\left(1 + \frac{[V]^n}{K_{is}{}^n}\right) + [AcCh_o]\left(1 + \frac{[V]^n}{K_{ii}{}^n}\right)} \quad (1)$$

which is a nonlinear noncompetitive equation in which V_{max} is defined by eq e of the Appendix, and

$$K_M = K_{Ao}\left(\frac{k_2 + k_{-2}}{k_1 + k_2}\right) \quad (2)$$

$$K_{ii}{}^n = K_{Vi}{}^n\left(1 + \frac{k_2}{k_1}\right) \quad (3)$$

and

$$K_{is}{}^n = K_{Vi}{}^n K_{Vo}{}^n \frac{(k_2 + k_{-2})}{(k_2 K_{Vi}{}^n + k_{-2} K_{Vo}{}^n)} \quad (4)$$

Preliminary values of the microscopic constants k_2 and K_{Vi} can be obtained from the macroscopic, regression-derived parameters for V_{max}, K_{ii}, and n by solution of eqs e and 3 if we assume that $[AcChT_t]$ is equal to $[VR_t]$, the total VR concentration, and that $k_1 \gg k_2$. The latter assumption is consistent with the observation that V_{max} does not depend on the structure of the transported ligand. Evidence presented by Rogers and Parsons (1992) demonstrates that $[AcChT_t]$ does not quite equal $[VR_t]$, but the error is small and will be ignored. The microscopic value of n is the same as the macroscopic value. Use of the regression parameters obtained with AcCh and methoxyvesamicol (Table II) yields the preliminary estimates $k_2 = 5.4\ min^{-1}$ and $K_{Vi} = 6.2\ \mu M$. In like manner, we estimate from parameters obtained with analogue 15 that $k_2 = 2.8\ min^{-1}$ and $K_{Vi} = 11\ \mu M$, and from analogue 14 that $k_2 = 1.6\ min^{-1}$ and $K_{Vi} = 13\ \mu M$.

The preliminary estimates of k_2 are quite low for a small molecule transporter. Many such transporters exhibit turnover numbers $>10^4\ min^{-1}$ (Wilson, 1978). This leads us to hypothesize that only a small fraction of the transporters in a typical vesicle preparation is competent in active transport. The hypothesis is supported more strongly below after we have fully developed our kinetics model. It explains much of the apparent complexity in the system that could not otherwise readily be reconciled with the allosteric model.

We also can extract approximate values for K_{Ao} and k_1. $K_{IA}{}^s$ and K_{IA} values state macroscopic affinities for AcCh

analogues that bind via the microscopic K_{Ao} and K_{Ai} steps. Exogenous analogue potentially can bind to inwardly oriented AcChT as such compounds equilibrate at equal concentration inside the vesicles under the conditions of the measurement (Carpenter et al., 1980; Noremberg & Parsons, 1989). As competition by an internal factor has been removed in ghosts, K_{IA}^{g} values more closely reflect intrinsic affinities of AcCh analogues for the AcChT. Thus, K_{IA}^{g}, and not K_{IA}, is appropriate for use in attempting to estimate microscopic affinities for AcCh analogues.

However, we must confront the following dilemma. The measurement of K_{IA}^{g} was carried out on resting AcChT-VR that probably was mostly active transport incompetent. Yet we are most interested in microscopic parameter values for actively cycling AcChT-VR. No experimental remedy is available to eliminate this gap in a rigorous analysis as we do not know how to isolate more competent vesicles.

The dilemma can be resolved approximately in the following manner. It is readily shown using Figure 6 that

$$K_{IA}^{g} = \frac{1 + k_{-2}^{i}/k_{2}^{i}}{1/K_{Ao}^{i} + (k_{-2}^{i}/k_{2}^{i})(1/K_{Ai}^{i})} \quad (5)$$

where the superscript i acknowledges that values of these constants in resting, transport-incompetent AcChT not exposed to endogenous factor apply. The addition of MgATP presumably does not affect the parameters because the macroscopic affinities of vesamicol and AcCh analogues are not affected significantly. The moderate decrease in B_{max} in some vesicle preparations that is seen in the presence of MgATP must be due to some other phenomenon. We can state that

$$k_{-2}^{i}/k_{2}^{i} = ck_{-2}/k_{2} \quad (6)$$

where c is the change in the ratio of k_{-2}/k_2 for the bulk of AcChT in resting ghosts relative to actively transporting AcChT in intact vesicles. The observation that AcCh analogues 23 and 25 exhibit no significant discrepancy between K_{IA}^{g} and IC_{50} values provides the information needed to proceed with the analysis. For a *nontransported* analogue, IC_{50} equals K_{Ao} in cycling AcChT. If we assume that analogues 23 and 25 are not transported (which is supported more below), the data in Table III for these analogues tell us that, after substituting eq 6 into eq 5,

$$K_{Ao} \cong K_{IA}^{g} = \frac{1 + ck_{-2}/k_{2}}{1/K_{Ao}^{i} + (ck_{-2}/k_{2})(1/K_{Ai}^{i})} \quad (7)$$

The simplest way in which eq 7 can be satisfied is where $ck_{-2} < k_2$ and $K_{Ao}^{i} < K_{Ai}^{i}$, so that $K_{Ao} \cong K_{IA}^{g} \cong K_{Ao}^{i}$.

K_{Ao}^{i} will equal K_{Ao} and K_{Ai}^{i} will equal K_{Ai} if transport-incompetent AcChT-VR is not damaged or otherwise modified at the AcCh-binding site. This would occur if the major cause of incompetency were lack of a proton motive force, perhaps due to damaged V-type ATPase, or to proton leaks. Indeed, preliminary evidence that poorly transporting vesicles contain little functional vacuolar-type ATPase has been obtained (B. Hicks, unpublished results). The relationships $k_{-2} < k_2$ and $K_{Ao} < K_{Ai}$ will promote inward active transport. The factor c will be 1 if the value of only the k_1 microscopic constant depends on the proton motive force and incompetent AcChT in ghosts is not different from competent AcChT in the rates of the k_2 and k_{-2} steps. We know that endogenous factor does not significantly inhibit otherwise competent AcChT, because active transport is nearly the same in resealed ghosts. We would expect a large increase in active transport by ghosts had this been the case. Thus, comparison of the properties of transport-competent AcChT in intact vesicles with those of the AcChT in ghosts is not complicated by endogenous factor. We discuss below what consequences ensue if $c \neq 1$.

Table IV: Calculated Microscope Constants[a]

AcCh analogue[b]	K_{Ao} (μM)[c]	k_1 (min^{-1})[c]	k_2 (min^{-1})	K_{Vi} (μM)[d]	n[d]
AcCh	50000	900	5.4	6.2	1.3
21[e]	6000	(200)	(5.4)		
15	700	40	3.0	11	1.6
14	2000	30	1.7	13	1.3
25[f]	1	0			
23[f]	2	0			

[a] Constants are defined by the model of Figure 6. Calculations utilized eqs e, 3, 7, and 8 as described in the text. [b] Structures of the analogues are shown in Table I. [c] One significant figure. [d] Values for methoxyvesamicol determined by inhibition of active transport of the indicated AcCh analogue. [e] The value of k_1 was estimated by assuming the value of k_2 obtained with AcCh and that IC_{50} equals K_M. [f] Assumed not to be actively transported.

Because of the reasonableness of the necessary assumptions and the economy of the result, we arrive at the conclusion that $K_{IA}^{g} \cong K_{Ao}$ for analogues 23 and 25. There is no reason to suppose that this is not general for all of the AcCh analogues, whether or not they are actively transported. We will take K_{IA}^{g}, rounded to one significant figure, as an estimate of K_{Ao} for all of them (Table IV). Values as low as 20 mM have been observed for AcCh in some studies (Noremberg & Parsons, 1989), but we will take the 50 mM value that was observed here.

A solvable expression for k_1 can be obtained by dividing eq 7 by eq 2 and making the same assumptions as above. This leads to

$$\frac{K_{IA}^{g}}{K_M} \cong \frac{k_1}{k_2} \quad (8)$$

Use of the data in Tables II and III, the preliminary estimates of k_2, and eq 8 yields, to one significant figure, estimates for k_1 of 900 min^{-1} for AcCh, 40 min^{-1} for analogue 15, and 30 min^{-1} for analogue 14 in the preparations of vesicles that were studied.

The estimate of k_1 now can be used in eqs e and 3 to obtain better estimates of k_2 and K_{Vi}. The iterated estimates do not change much and are listed in Table IV. The success of the kinetics model for AcCh, analogue 14, and analogue 15 leads us to predict that all analogues of AcCh that exhibit significantly lower IC_{50} compared to K_{IA}^{g} values are actively transported. This is a useful inference, as it is expensive to synthesize radiolabeled analogues for direct measurement of K_M values. Thus, we have used the value of k_2 determined from the AcCh study and the K_{IA}^{g}/IC_{50} ratio for analogue 21 (Table III) to compute k_1 for analogue 21 (Table IV).

The k_1 values are significantly larger than k_2 for transported analogues, confirming the assumption that the rate-limiting step of active transport is k_2. The observation that the estimated values of k_2, K_{Vi}, and n were not constant in the different transport experiments is not surprising in view of the substantial variation in the properties of the AcChT-VR in different preparations of vesicles. The 2-fold lower V_{max} for analogues 14 and 15 relative to AcCh found for some preparations of vesicles (Clarkson et al., 1992) could arise from nonequilibrium binding of the analogues, perhaps because the K_{Ao} step actually is complex. The reasons for the variations that have been observed are not known, but evidence that the system is regulated has been presented (Gracz et al., 1988). The macromolecular structure observed for the AcChT-VR in the following papers is heterogeneous, and such a structure seems uniquely suited to variability.

On a conceptual level, the K_M values for transported analogues are as much as 200-fold lower than the estimated K_{Ao} values because rapid inward transport increases the fraction of transporter that apparently (to an outside observer) is occupied. For AcCh, this effect reduces the transport Michaelis constant to below the physiological concentration of about 4 mM that can be estimated for electromotor terminal cytoplasm (Morel et al., 1978; Weiler et al., 1982).

While specific values for the other microscopic constants in the model cannot be estimated from the available data, deductions about the relative values of some of them can be made nevertheless. Methoxyvesamicol must bind with higher affinity to the outwardly oriented competent transporter. If one takes the ratio of eq 4 to eq 3, it can be seen that the resulting relationship mathematically requires that $K_{Vo} < K_{Vi}$ in order to generate $K_{is} < K_{ii}$. It was this realization that led to postulation of the V_n·VR′–AcChT$_o$ complex in the model (Figure 6). This deduction was not possible on the basis of the data obtained from inhibition of AcCh active transport by vesamicol, as the errors in the K_{is} and K_{ii} values were too large. We already have hypothesized that $k_{-2} < k_2$ and $K_{Ao} < K_{Ai}$. We can get no information about k_{-1} as it does not operate because either $K_{Ai} = \infty$ or [AcCh$_i$] = 0 for transport-competent AcChT–VR.

Development of the kinetics model allows us to analyze the effect that active transport will have on the affinity of ligands. Resting AcChT–VR will bind vesamicol analogues primarily to outwardly oriented transporter if $k_{-2} \leq k_2$, whereas transporting AcChT–VR will bind vesamicol analogues primarily to inwardly oriented transporter because that is the major form present when $k_1 > k_2$. As we have concluded that competent transporter oriented inwardly binds methoxyvesamicol with less affinity than when oriented outwardly, the macroscopic affinity of vesamicol analogues should decrease upon activation of transport. However, there is no significant effect in the K_M concentration range of AcCh (Noremberg & Parsons, 1989; Figure 5). Similarly, initiation of active transport has no effect on the apparent affinity of AcCh as measured by inhibition of [^{3}H]vesamicol binding (Noremberg & Parsons, 1989), despite our conclusion above that the affinity for AcCh increases 100–200-fold in cycling AcChT. Both behaviors clearly suggest that most of the AcChT–VR in purified vesicles is transport incompetent, in agreement with the low values of k_2. The observation that vesamicol analogues inhibit active transport at concentrations that only partially occupy the VR (Kaufman et al., 1989; compare K_{ii} and K_{is} values in Table II to K_{IV} values in Figure 5) can be reconciled to this conclusion by hypothesizing that a small fraction of transport-component AcChT–VR binds vesamicol analogues more tightly than a large excess of transport-incompetent AcChT–VR. There appears to be something different about the structure of the VR in competent AcChT. This correlates with the ability of internal endogenous factor to inhibit binding of AcCh to transport-incompetent but not competent AcChT–VR.

A large proportion of transport-incompetent AcChT–VR in the vesicle preparations affects estimates of the microscopic constants in the following ways. K_{Vi} and n are not affected. The calculated value of k_2 is too low by the fraction of transport-incompetent AcChT–VR. If only 10^{-4} of the AcChT–VR was competent in the experiment in Figure 1, then the corrected value of k_2 is 54 000 min^{-1}. If $c < 1$, then the estimated K_{Ao} is too high by a factor of up to about $(1 + k_{-2}/k_2)$, but for $k_{-2} \lesssim k_2$, this will be a several-fold error at most. It seems unlikely that $c < 1$ as that would represent a relatively larger k_{-2}/k_2 ratio in competent transporter that is less favorable for active transport. If $c > 1$, then the estimated K_{Ao} is too low by a factor of up to about $(1 + k_2/k_{-2})/c$. This would occur if the k_2 microscopic constant depends on the proton motive force. In this case, we will have underestimated the extent to which the substrate binding properties of the AcChT–VR are extraordinary. Thus, the assumption that $c = 1$ is robust and reasonable and cannot lead to a significant conceptual error in our model. The values of k_1 are too low by the fraction of transport-incompetent AcChT–VR and are possibly further subject to relatively small error caused by the assumptions that $c = 1$ and $K_{Ao}{}^i = K_{Ao}$. Corrected k_1 will approximately scale with k_2, ensuring that it remains large relative to k_2. In summary, the estimates of the microscopic constants for equilibrium steps are approximately correct, but those for rate steps are too low by unknown similarly large factors. *Relative* values of k_1 for different transported analogues of AcCh can be compared with each other in an approximate sense *if* we normalize the k_1 values to the same apparent, analogue-independent values of k_2. The value of k_1 obtained from the analogue 14 study would have been about 100 min^{-1} had the vesicles transported AcCh as well as the preparation used in the full AcCh study. Analogue 14 was transported only about 9-fold more slowly than AcCh in the actual uptake step, and this had no effect on the V_{max}.

The mechanism of the allostery and noncompetitive inhibition of active transport that is shown by the vesamicol family requires comment. In the model presented here, only binary complexes are hypothesized. Vesamicol or any other compound that binds to the VR will trap the AcChT in an unproductive complex without the necessity of inducing a propagated conformational change. This explains how structurally unrelated drugs, which are unlikely to induce similar conformational changes, all can inhibit active transport of AcCh by acting on the VR. In the macroscopic kinetics, vesamicol is noncompetitive during active transport because it can bind to inwardly oriented (empty) transporter generated from AcChT$_o$·AcCh$_o$ by the k_1 and K_{Ai} steps. Thus, in the steady state, vesamicol *appears* to bind to the AcChT·AcCh complex, even though a ternary complex never is formed.

It is clear for the following two reasons that the AcChT does not engage in tight, precise contact with transported analogues. First, although AcCh is small, it has enough structure to produce tight binding to proteins, as the desensitized complex with the nicotinic receptor has a dissociation constant of about 10 nM (Prinz & Veltel, 1988). The affinity for the AcChT is at least 10^6-fold less. Second, the previous structure–activity study of AcCh analogue binding demonstrated that the pharmacophores are the carbonyl and quaternary ammonium groups (Rogers & Parsons, 1989). Beyond those features, increased hydrophobicity increases the affinity, but the shape of the additional bulk in the analogue is not very important. We now know that analogues containing extra steric bulk in five- and six-membered rings connecting the pharmacophores (analogues 14 and 15 compared to 21) and on either side (analogue 14 compared to 15) are actively transported. Morever, previous work with intact cholinergic preparations had demonstrated that acetyltriethylcholine and acetylhomocholine are actively transported (Collier, 1986; Newton & Jenden, 1986). This is an extraordinarily diverse range of substrates, and it is very unlikely that a lock-and-key mechanism for substrate recognition by the AcChT would accept all of these substrates.

In order to examine the steric space occupied by actively transported substrates in more detail, we have constructed a

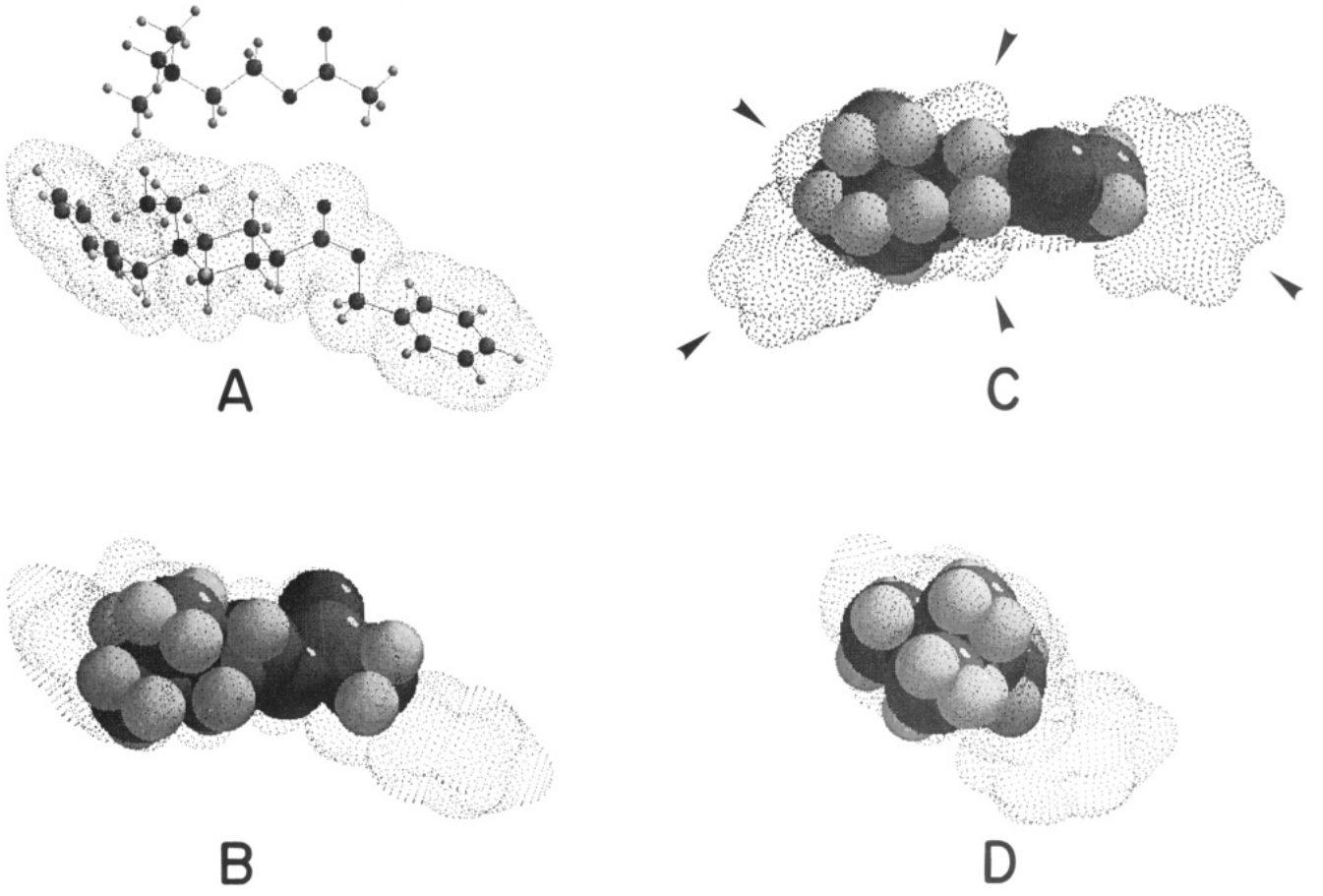

FIGURE 7: Overlay of AcCh onto a chimeric analogue constructed from the features of transported analogues. The chimera is *trans*-benzyl *N*-benzyl-*N*-ethylisonipecotate. The conformations of AcCh and the chimera were energy-minimized using the MM2P subroutine of CHEM-X. The structures are shown as ball-and-stick models in panel A, with a transparent van der Waals surface surrounding the chimeric model. The orientation is similar to the structures in Table I, with the quaternary amines toward the left. In panels B, C, and D, the quaternary amines and carbonyl groups were superimposed as closely as possible, and the solid van der Waals surface of AcCh is shown embedded in the transparent van der Waals surface of the chimera. In AcCh the N to carbonyl O distance is 4.959 Å, and in the chimera it is 4.660 Å. Panel B is the side view corresponding to panel A that is perpendicular to the plane of the AcCh carbonyl, panel C is the top view parallel to the axis of the AcCh carbonyl with the oxygen atom facing the viewer, and panel D is the end-on view with the quaternary amine facing the viewer. The regions of substantial extra steric space occupied by the chimera are indicated by the arrow heads.

hypothetical chimeric AcCh analogue that incorporates many of the chemical features that are individually accepted by the AcChT. The chimera incorporates the six-membered piperidine ring of analogue 21, the phenyl groups of analogues 14 and 15, and the ethyl groups of acetyltriethylcholine. The conformations of AcCh and the chimera were energy-minimized about the probable conformation of AcCh bound to the transporter that was determined by Rogers and Parsons (1989). This *trans–trans* conformer for AcCh is observed during molecular dynamics in water, indicating that it indeed is relatively stable (Edvardsen & Dahl, 1991). The resulting energy-minimized structures are superimposed in Figure 7. There are five regions of substantial additional steric space distributed around the AcCh molecule (best seen in Figure 7C) that are occupied by the different transported substrates. The pharmacophores are accessible through restricted regions of the van der Waals surface, so that a recognition mechanism based on weak interactions still could operate. However, an active transporter making close contacts with its substrate is very unlikely to accept such a punctate envelope of steric hindrances around the pharmacophores during all stages of the transport event.

The very weak affinity for AcCh and low substrate specificity observed here suggest that the AcChT might be channel-like. Such a structure probably must have two reciprocally controlled gates that define an internal chamber where substrate is bound loosely in order to account for active transport and not allow leakage of protons. The outside and inside orientations of the transporter indicated in Figure 6 would correspond to closed states of the inside and outside gates, respectively. We hypothesize that transported AcCh analogues can assume extended, approximately linear shapes that are not too long or too wide to fit into the hypothetical sealed internal chamber. Analogues 23 and 25 apparently are too long, although they still can bind to the chamber when it is open to the outside. Similar analogues have been synthesized in tritiated form and directly shown to be actively transported very poorly or not at all (Clarkson et al., 1992; Rogers & Parsons, 1992). Moreover, the recognition sites for the pharmacophores must accept a variable spacing, as acetylhomocholine is transported. This too is consistent with a weak interaction between the hypothesized chamber and transported substrates. Alternatively, the kinetics and low specificity for substrate resemble the properties of the multidrug transporter, which recently was proposed to be a "flippase" acting on molecules that intercalate into a bilayer leaflet (Higgins & Gottesman, 1992).

Although the AcChT exhibits very low specificity, it does not totally lack specificity. Acetyldiethylhomocholine is an abortive false transmitter in mammalian brain and sympathetic ganglion (Welner & Collier, 1984, 1985), failing at the storage step, and we have just concluded that the AcCh analogues

containing significant steric bulk on both ends are not actively transported by synaptic vesicles purified from electric organ. Too many simultaneous increases in steric bulk exceed the accommodation that the transporter can make to them individually. Even transported analogues exhibit lower values of k_1 relative to AcCh, meaning that they do not pass as freely through the AcChT as AcCh. This is consistent with a model where the diameter of the analogues approaches the smallest diameter of the pathway through the AcChT.

Presumably the AcChT has these special properties for a purpose. This could be a requirement for very fast transport and release. Very fast transport would be required for rapid mobilization of cytoplasmic AcCh during high frequency evoked release. This would require very fast release that also ensures that K_{Ai} is very large so that the net rate of transport does not slow excessively as $AcCh_i$ approaches its final concentration of about 0.5–0.9 M in fully loaded vesicles (Morris, 1980). The same fast-kinetics requirement faces nerve terminals that utilize other neurotransmitters. Dopamine, serotonin, histamine, epinephrine, and norepinephrine all are actively transported by the reserpine-sensitive vesicular transporter (Johnson, 1988). The very low specificity of this transporter is consistent with a channel- or flippase-like structure requiring only aromatic and amine pharmacophores in its substrates. Similarly, γ-aminobutyric acid (GABA) and glycine, which have very different van der Waals volumes, probably are transported by a single vesicular transporter (Christensen et al., 1991; Burger et al., 1991). The kinetics properties of the AcChT deduced here are well suited to its physiological role in storage of neurotransmitter, and they might have general utility for other neurotransmitter storage systems.

Acknowledgments

We thank Catherine Fehlmann, Daniel Oros, and Wendy Connelly for isolation of synaptic vesicles and Larry M. Gracz for improvements in the isolation process. We are especially grateful to Professor Roger C. Millikan for carrying out molecular graphics calculations.

Appendix: Expression for Rate of AcCh Transport and Inhibition by Vesamicol

The rate expression for AcCh transport by the scheme shown in Figure 6 can be derived by the King–Altman procedure as simplified by Cha (1968) for reactions containing steps at equilibrium. The species on the top line can be grouped to form composite 1. The species on the bottom line form composite 2. The rate of the reaction $VR'\text{–}AcChT_o\cdot AcCh_o \rightarrow VR\text{–}AcChT_i\cdot AcCh_i$ is $k_1[VR'\text{–}AcChT_o\cdot AcCh_o]$. But since $VR'\text{–}AcChT_o\cdot AcCh_o$ is in equilibrium with $VR'\text{–}AcChT_o$ and $V_n\cdot VR'\text{–}AcChT_o$, its concentration can be written as a fraction of the composite 1 concentration equal to

$$A = [1 + K_{Ao}/[AcCh_o] + K_{Ao}[V]^n/([AcCh_o]K_{Vo}^n)]^{-1}$$

Similarly, the concentration of $VR\text{–}AcChT_i\cdot AcCh_i$ can be written as a fraction of composite 2 equal to

$$B = [1 + K_{Ai}/[AcCh_i] + [V]^n K_{Ai}/([AcCh_i]K_{Vi}^n)]^{-1}$$

For $VR\text{–}AcChT_i$,

$$C = (1 + [V]^n/K_{Vi}^n + [AcCh_i]/K_{Ai})^{-1}$$

and for $VR'\text{–}AcChT_o$,

$$D = (1 + [AcCh_o]/K_{Ao} + [V]^n/K_{Vo}^n)^{-1}$$

The transporter reorientation reactions of Figure 6 then can be rewritten as

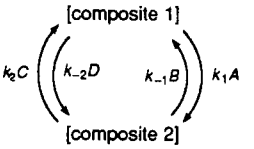

The rate of AcCh transport is given by

$$\frac{d[AcCh_i]}{dt} = \text{rate} = k_1A[\text{composite 1}] - k_{-1}B[\text{composite 2}] \quad \text{(a)}$$

The fraction of the total transporter $[AcChT_t]$ that is present in composite 1 is given by the sum of the effective rate constants of all processes producing composite 1 divided by the sum of the effective rate constants of all processes producing composites 1 and 2. Thus,

$$[\text{composite 1}] = [AcChT_t]\left(\frac{k_{-1}B + k_2C}{k_1A + k_{-1}B + k_2C + k_{-2}D}\right) \quad \text{(b)}$$

An analogous expression holds for composite 2.

$$[\text{composite 2}] = [AcChT_t]\left(\frac{k_1A + k_{-2}D}{k_1A + k_{-1}B + k_2C + k_{-2}D}\right) \quad \text{(c)}$$

Substituting eqs b and c into eq a gives

$$\frac{\text{rate}}{[AcChT_t]} = \frac{k_1A(k_{-1}B + k_2C) - k_{-1}B(k_1A + k_{-2}D)}{k_1A + k_{-1}B + k_2C + k_{-2}D} \quad \text{(d)}$$

The rate can be referenced to the maximal rate V_{max} by computing $\text{rate}/[AcChT_t]$ when $[AcCh_o] \gg K_{Ao}$, $[AcCh_i] = 0$, and $[V] = 0$. Under these conditions, $A = C = 1$, $B = D = 0$, and

$$\frac{V_{max}}{[AcChT_t]} = \frac{k_1k_2}{(k_1 + k_2)} \quad \text{(e)}$$

Division of eq d by eq e gives

$$\frac{\text{rate}}{V_{max}} = \left[\frac{k_1A(k_{-1}B + k_2C) - k_{-1}B(k_1A + k_{-2}D)}{k_1A + k_{-1}B + k_2C + k_{-2}D}\right]\frac{(k_1 + k_2)}{k_1k_2} \quad \text{(f)}$$

With suitable initial velocity simplification and gathering of terms, the last equation can be recast into the Michaelis–Menten form shown in the text as eq 1.

Registry No. AcCh, 51-84-3; vesamicol, 22232-64-0; (±)-*trans*-6-methoxyvesamicol, 120447-25-8; methyl 1,1-dimethylisonipecotate iodide, 51023-67-7; (±)-1,1-dimethyl-3-benzoyloxypyrrolidinium iodide, 124805-68-1; (±)-*cis*-1-benzyl-1-methyl-3-acetoxypyrrolidinium bromide, 141434-91-5; (±)-*trans*-1-benzyl-1-methyl-3-acetoxypyrrolidinium bromide, 141434-92-6; *cis*-cyclopentylmethyl 1-benzyl-1-methylisonipecotate bromide, 141376-35-4; *trans*-cyclopentylmethyl 1-benzyl-1-methylisonipecotate bromide, 141376-36-5; *cis*-benzyl 1-benzyl-1-methylisonipecotate bromide, 124805-73-8.

References

Anderson, D. C., King, S. C., & Parsons, S. M. (1982) *Biochemistry 21*, 3037–3043.

Anderson, D. C., King, S. C., & Parsons, S. M. (1983) *Mol. Pharmacol. 24*, 48–54.

Anderson, D. C., Bahr, B. A., & Parsons, S. M. (1986) *J. Neurochem. 46*, 1207–1213.

Bahr, B. A., & Parsons, S. M. (1986a) *J. Neurochem. 46*, 1214–1218.

Bahr, B. A., & Parsons, S. M. (1986b) *Proc. Natl. Acad. Sci. U.S.A. 83*, 2267–2270.

Bahr, B. A., & Parsons, S. M. (1989) in *Receptors, Membrane Transport and Signal Transduction* (Evangelopoulos, E. A., Changeux, J. P., Packer, L., Sotiroudis, T. G., & Wirtz, K. W. A., Eds.) NATO ASI Series, Vol. 29, pp 233–241, Springer-Verlag, Berlin.

Bahr, B. A., & Parsons, S. M. (1992) *Biochemistry* (second paper of four in this issue).

Bahr, B. A., Noremberg, K., Rogers, G. A., Hicks, B. W., & Parsons, S. M. (1992) *Biochemistry* (fourth paper of four in this issue).

Bradford, M. M. (1976) *Anal. Biochem. 72*, 248–254.

Burger, P. M., Hell, J., Meht, E., Krasel, C., Lottspeich, F., & Jahn, R. (1991) *Neuron 7*, 287–293.

Carpenter, R. S., Koenigsberger, R., & Parsons, S. M. (1980) *Biochemistry 19*, 4373–4379.

Cha, S. (1968) *J. Biol. Chem. 243*, 820–825.

Christensen, H., Fykse, E. M., & Fonnum, F. (1991) *Eur. J. Pharmacol. 207*, 73–79.

Clarkson, E. D., Rogers, G. A., & Parsons, S. M. (1992) *J. Neurochem.* (in press).

Cleland, W. W. (1979) *Methods Enzymol. 63*, 103–138.

Collier, B. (1986) *Can. J. Physiol. Pharmacol. 64*, 341–346.

Edvardsen, O., & Dahl, S. G. (1991) *J. Neural Transm. 83*, 157–170.

Gracz, L. M., Wang, W.-C., & Parsons, S. M. (1988) *Biochemistry 27*, 5268–5274.

Higgins, C. F., & Gottesman, M. M. (1992) *Trends Biochem. Sci. 17*, 18–21.

Johnson, R. G. (1988) *Physiol. Rev. 68*, 232–307.

Kaufman, R., Rogers, G. A., Fehlmann, C., & Parsons, S. M. (1989) *Mol. Pharmacol. 36*, 452–458.

Kornreich, W. D., & Parsons, S. M. (1988) *Biochemistry 27*, 5262–5267.

Marshall, I. G., & Parsons, S. M. (1987) *Trends Neurosci. 10*, 174–177.

Morel, N., Israel, M., & Manaranche, R. (1978) *J. Neurochem. 30*, 1553–1557.

Morris, S. J. (1980) *Neuroscience 5*, 1509–1516.

Newton, M. W., & Jenden, D. J. (1986) *Trends Pharmacol. Sci. 7*, 316–320.

Noremberg, K., & Parsons, S. M. (1989) *J. Neurochem. 52*, 913–920.

Parsons, S. M., Noremberg, K., Rogers, G. A., Gracz, L. M., Kornreich, W. D., Bahr, B. A., & Kaufman, R. (1988) in *Cellular and Molecular Basis of Neuronal Signaling* (*Synaptic Transmission*) (Zimmermann, H., Ed.) pp 325–335, Springer-Verlag, Berlin.

Prinz, H., & Veltel, D. (1988) *Biol. Chem. Hoppe-Seyler 369*, 1243–1249.

Rogers, G. A., & Parsons, S. M. (1989) *Mol. Pharmacol. 36*, 333–341.

Rogers, G. A., & Parsons, S. M. (1992) *Biochemistry* (third paper of four in this issue).

Rogers, G. A., Parsons, S. M., Anderson, D. C., Nilsson, L. M., Bahr, B. A., Kornreich, W. D., Kaufman, R., Jacobs, R. S., & Kirtman, B. (1989) *J. Med. Chem. 32*, 1217–1230.

Weiler, M., Roed, I. S., & Whittaker, V. P. (1982) *J. Neurochem. 38*, 1187–1191.

Welner, S. A., & Collier, B. (1984) *J. Neurochem. 43*, 1143–1151.

Welner, S. A., & Collier, B. (1985) *J. Neurochem. 45*, 210–218.

Wilson, D. B. (1978) *Annu. Rev. Biochem. 47*, 933–965.